Link between structural and mechanical stability of fcc- and bcc-based ordered Mg-Li alloys.

M.J. Phasha[1,2], P.E. Ngoepe[1,2] and H.R. Chauke[1]

[1]*Materials Modelling Center, School of Physical and Minerals Sciences, University of Limpopo, Private Bag x1106, Sovenga, South Africa*

[2]*Materials Science and Manufacturing, CSIR, Meiring Naude, Brummeria, P.O. Box 395, Pretoria 0001, South Africa*

D.G. Pettifor[3]

[3]*Materials Modelling Laboratory, Department of Materials, University of Oxford, Parks Road, Oxford, OX1 3PH UK*

D. Nguyen-Mann[4]

[4]*UKAEA, Culham Science Centre, Oxfordshire, OX14 3DB, UK*

Abstract

The first principles pseudopotential calculations based on the Perdew-Burke-Ernzerhof (PBE) form of generalized gradient approximation (GGA) within density functional theory (DFT) have been utilized to investigate the structural and elastic properties of cubic-based Mg-Li alloys. The heats of formation and elastic moduli were used in predicting structural stability profile, and their results are consistent with each other. In terms of phase stability, an interesting correlation between the calculated tetragonal shear modulus (C') and formation energy of corresponding bcc and fcc ordered compounds relative to hcp Mg and Li lattices is drawn. The predicted stability trend due to structural energy difference was further confirmed by electronic structure calculations based on Jones-type analysis.

Corresponding author: mphasha@csir.co.za

1. Introduction

Magnesium is one of the readily available metals, constituting about 2.7% of earth's crust, offers several advantages including excellent machinability, recyclability, good castability, good weldability, good creep resistance, high thermal conductivity, and extreme lightness [1]. These features render magnesium alloys suitable and ideal for use in applications where lightweight to specific strength ratio is vital. At a density of 1.74 g/cm³, magnesium (Mg) is amongst others the lightest structural metal. However, due to hexagonal close-packed (hcp) crystal structure, Mg and Mg alloys have undesirable mechanical properties at room temperature, including difficult workability. Fortunately, the addition of at least 11 weight percent (wt.%) lithium does not only reduce the density of magnesium but also transforms the hcp Mg into more workable body-centred cubic (bcc) phase [2]. The resulting magnesium-lithium (Mg-Li) alloys exhibit good formability and becomes the lightest metallic alloys with promising technological applications in transport (automotive and aerospace) and communication (portable electronic equipments) industries, due to their good strength-to-weight ratio and improved ductility. Furthermore, the existence of metastable fcc (face-centered cubic) at concentrations between 15 and 35 atomic percent (at.%) Mg has been predicted in the past, at least at very low temperatures [21].

Currently, the development of Mg alloys with desirable physical and mechanical properties with remarkable weight saving application remains a challenge. If the development of these alloys follows a path similar to Al alloys [3], using traditional trial and error methods and techniques, it would require a similar level of effort of many years. However, *ab initio* density functional theory (DFT) methods provide an opportunity to drastically accelerate materials research by efficiently predicting new phases and accurately describing their ground states [4]. Recently, *ab initio* calculations have concentrated on gaining a detailed knowledge of the electronic structure of materials and its effects on microscopic and macroscopic behaviours [5,6]. Considering these simulation advantages, the theoretical *ab initio* studies on Mg-Li system remain surprisingly scarce [7,8,9]. The work by Uesugi et al focused only on hcp Mg_7Li alloy [7,8], while the more recent investigation by Counts et al emphasized the mechanical properties of only bcc Mg-Li alloys using the supercell approach [9].

In this paper, the *ab initio* calculations based on pseudopotentials plane wave method were used to investigate existence of fcc and bcc binary Mg-Li alloys at 0 K for various concentrations, using ordered crystal structures. In order to avoid unworkable hcp Mg alloys, the current work attempts to find suitable alternative stable or metastable cubic low temperature formable Mg-Li alloys, from heats of formation. Furthermore, we investigate if these cubic phases possess desirable mechanical properties and are easily malleable. The current work focuses on cubic Mg-Li ordered structures within 3:1 ($L1_2$ and DO_3) and 1:1 ($L1_0$ and B2) stoichiometries, while the end elements were taken as fcc

3

and bcc for both Mg and Li. In order to study small additions of Mg and Li to pure Li and Mg metals respectively, we also examine the 7:1 and 15:1 stoichiometry in the fcc and bcc lattice, respectively. We will find which phases are more stable based on the predicted negative heats of formation and the structural formation difference ($\triangle H_f$ (bcc-fcc)). Furthermore, the mechanical stability for cubic crystals will be determined from tetragonal shear modulus, while elastic moduli and ratio of bulk to shear modulus (measure of ductility) will also be reported. Moreover, we will note the correlation on the trend of structural formation difference ($\triangle H_f$ (bcc-fcc)) and change in shear modulus ($\triangle C'$). In order to validate the phase stability in terms of structural energy differences, the electronic structure (ES) calculations due to electron band filling (electron per atom ratio) spanning the entire concentration range of fcc and bcc phases will be determined. ES was based on rigid-band model formalized by Jones-type analysis, and therefore provides composition ranges in which cubic phases are stable.

This paper is organized as follows, in Sec. 2, the computational details followed to solve the electronic structure are briefly outlined. The trends in cohesive and elastic properties are respectively analysed and discussed in Sec. 3. Finally, Sec. 4 presents the conclusion of the paper.

2. Computational details

The equilibrium lattice parameters and electronic structure calculations were optimized using the *ab-initio* plane wave (PW) pseudopotential method, embodied in the CASTEP code [10]. The Hohenberg-Kohn-Sham density functional theory (DFT) [11] was used

within the GGA formalism [12] to describe the electronic exchange-correlation interactions. We used the recent PBE form of the GGA [13], which was designed to be more robust and accurate than the original GGA formulation. The Vanderbilt ultrasoft pseudopotentials [14], were employed for Mg-Li structures. Calculations were carried out on ordered fcc-based phases, $L1_2$ ($MgLi_3$, Mg_3Li, and ($MgLi_7$, Mg_7Li) and the bcc-based phases B2 (MgLi), B32 (MgLi), DO_3 ($MgLi_3$), Mg_3Li) and ($MgLi_{15}$, $Mg_{15}Li$). In addition, the structural energetics of tetragonal $L1_0$ (MgLi) and DO_{22} ($MgLi_3$, Mg_3Li) phases are reported. The first set of calculations were performed at our theoretically determined (equilibrium) lattice constants for each structure [15], with a plane-wave basis set defined by an energy cut-off of 500 eV for all considered superstructures. Furthermore, the minimum and maximum Guassian smearing width were respectively set at 0.4 and 0.1 eV for superstructures, and at 0.1 and 0.01 eV for elemental metals, since the lattices of the latter involves energy differences of the order 1 to 100 meV/atom than is required in the former. In addition, this condition requires the use of denser Monkhorst-Pack [16] sets of **k**-points and a little alteration to the defaulted setting within the code, especially in case of Li, than it is averagely and adequately acceptable, respectively, for Mg and alloyed compounds. These parameters are essential since the Fermi energy, and hence the total energy depends quite sensitively on them. The convergence criterion of less than 2×10^{-5} eV on total energy per atom, 10^{-3} Å on the displacement of atoms, 0.05 eV/Å on the residual forces, and 0.1 GPa on the residual bulk stress was used. Uncommonly, a special care was taken when treating Li element, only during structure relaxations to avoid emanating stable phase disagreements with experiments. With our choice of mesh grid in the full Brillouin zone, the selected sufficient cut-off energy and **k**-points were converged

to within 1 meV/atom and 5 meV/atom for pure elements and superstructures, respectively.

The second set of calculations was performed to obtain elastic coefficients of Mg-Li alloys using CASTEP on Materials Studio version 3.0 interface [17]. We used six different values of the strain ±0.0008, ±0.0024 and ±0.004 for each structure. The application of strain on the lattice implies a lowering of symmetry from that of the crystal, therefore very accurate total-energy calculations are required, since the energy differences involved are of the order 10 to 1000 µeV/atom. In addition, this condition requires the use of slightly denser **k**-points to be utilized than in geometry optimization of crystals. The current set of calculations was considered converged when the maximum force on atoms was below 0.01 eV/Å, the total energy change per atom was less than 4×10^{-4} eV/atom and the displacement of atoms was below 4×10^{-4} Å. The value of the stress was automatically computed for each strain, and resulted in a stress-strain linear fit curve, from which each component of the stress was computed, and respective gradients provided the values of the corresponding elastic constants. Based on three independent single crystal elastic constants of a cubic crystal, C_{11}, C_{12}, C_{44}, , the elastic moduli of polycrystalline material were calculated following averaging schemes of Voigt (upper bound) and Reuss (lower bound) as follows [28]:

$$E = \frac{9BG}{3B+G}, \ G = \frac{1}{2}\left[\frac{C_{11} - C_{12} + 3C_{44}}{5} + \frac{5C_{44}(C_{11} - C_{12})}{4C_{44} + 3(C_{11} - C_{12})}\right]$$

$$B = \left(\frac{C_{11} + 2C_{12}}{3}\right), \ C' = \frac{C_{11} - C_{12}}{2}, \ A = \frac{(2C_{44} + C_{12})}{C_{11}}$$

where E is the Young's modulus, G shear modulus, B bulk modulus, C' tetragonal shear modulus and anisotropic factor A.

3. Results and discussions

3.1. Structural stability

The equilibrium lattice parameter, a_0, of the geometrically optimized structures are listed in Table I. In calculations where the ordered superstructures were used, resulting to twice the value of a_0, the calculated a_0 values listed in Table 1 were normalized, for comparison purposes. With increasing Li concentration, the lattice parameter decreased to its minimum at 50:50 equi-atomic compositions, after which a slight increase in a_0 is observed. The observed trend, which deviates slightly from Vegard's law for solid solutions, is similar in both bcc and fcc Mg-Li alloys considered in this study. This behaviour was also realised in earlier theoretical [18,21] as well as experimental [19,20] studies. Although the lattice parameter of bcc Li is underestimated by current and other calculations [36,37], in general our predicted lattice parameters are in good agreement with available experimental and theoretical results.

The heat of formation, H_f, of the alloy is computed according to the relation

$$H_f^{Mg_{1-x}Li_x} = \frac{1}{n} E_{total}^{Mg_{1-x}Li_x} - \left[(1-x)E_{solid}^{Mg} + xE_{solid}^{Li} \right] \tag{1}$$

where $E_{total}^{Mg_{1-x}Li_x}$ is the total energy of the alloy, E_{solid}^{Mg} and E_{solid}^{Li} are the total energies of the stable structures of elemental Mg and Li, n is the total number of atoms in the superstructure, x and $(1-x)$ refers to the fractional concentrations of the constituent elements.

We note that the heat of formation curve shown in Figure 1 makes a V-shape, with its minimum at the equi-atomic concentration of MgLi compound. At 50-50 concentration, the B2 structure is clearly the most stable phase, since it has the lowest formation energy amongst its competing counterparts. The calculations predict the B2 structure to be 26.0 meV/atom lower in energy compared to B32 phase. Our predicted heat of formation for the B2 structure of -73.4 meV/atom is in excellent agreement with Skriver's DFT result of -73.5 meV/atom [18], and is thus consistent with earlier experimental observations regarding tendency towards B2 (CsCl) type ordering at low temperatures [19,20]. The $L1_0$ structure, which was relaxed from c/a=1, collapses to c/a=0.72. This is because the tetragonal system is not stationary by symmetry for c/a=1 but collapses down to B2 with c/a=0.707. The frozen $L1_0$ with c/a=1 lies 29.25 meV/atom higher in energy compared to B2 phase.

The heat of formation for Mg_3Li alloy composition was calculated for three equivalent ordered crystal structures (DO_3, $L1_2$, DO_{22}) as shown in Figure 1. It clearly shows the preferred stability of the DO_3 phase over the $L1_2$ and DO_{22} phases, with formation energies of -38.32, -23.96 and -18.82 meV/atom, respectively. Our predicted phase stability ordering is the same as that of Skriver [18]. However, in the $MgLi_3$ compound, the DO_{22} structure has the lowest formation energy (-37.43 meV/atom) with the $L1_2$ and DO_3 phases lying only 0.82 and 6.32 meV/atom higher, respectively, in contrast to Skriver. We see that Skriver predicts the DO_3 phase to be more stable than DO_{22}. This is probably because their c/a axial ratio was not relaxed from its ideal value of 2.00, as

compared to our relaxed equilibrium value of 2.02. The slight difference between $L1_2$ and DO_{22} indicates a strong stability contest between these phases.

The solid common tangent lines were constructed in Figure 1 to show the stability limits of the different phases. Among the structures considered, the most energetically favourable intermetallic phases at absolute zero are the DO_3 Mg_3Li, B2 MgLi, DO_{22} and $L1_2$ $MgLi_3$ and $MgLi_7$ compounds. The DO_3 structure is metastable at 25 at.% Li, while the B32 and $L1_0$ structures are metastable at 50 at.% Li. Our equilibrium calculations predict DO_3 to be the most stable structure at A_3B (Mg–rich) composition, while at Li-rich side (AB_3) the face-centered structures ($L1_2$ and DO_{22}) show more stability over the body-centered phase.

The Mg-rich compounds, the bcc supercell $Mg_{15}Li$ and the fcc supercell Mg_7Li, lie well above the tangent line connecting hcp Mg ($H_f = 0$ eV) with DO_3 Mg_3Li. This clearly indicates the instability of the bcc and fcc Mg-Li compounds around this region. This instability supports Hafner's earlier work [21] that hcp Mg-Li compounds are dominant in the region with less than 18 at.% Li concentration. The formation energy of Mg_3Li in both the DO_{22} and $L1_2$ structures lie above tangent line, which indicates the instability of the fcc lattice in this region. Most of Mg-Li compounds at the Li-rich side lie either exactly or very close to the tangent line connecting B2 MgLi with elemental hcp Li. For example, fcc $MgLi_7$ shows a strong sign of metastability as it was earlier pointed [21]. Thus, low temperature sequence of hcp $\rightarrow$ bcc $\rightarrow$ hcp alloy phases with the existence of metastable fcc phase in Li-rich dual phase region is predicted, resulting to possible hcp $\rightarrow$ fcc $\rightarrow$ bcc $\rightarrow$ hcp stability trend. Structural formation energy differences, ΔH_f,

between corresponding bcc and fcc Mg-Li compounds, against the electron per atom ratio, as illustrated in Figure 2(a) also suggest the same trend. The above predicted stability profile is in full agreement with both experimental as well as theoretical results [21].
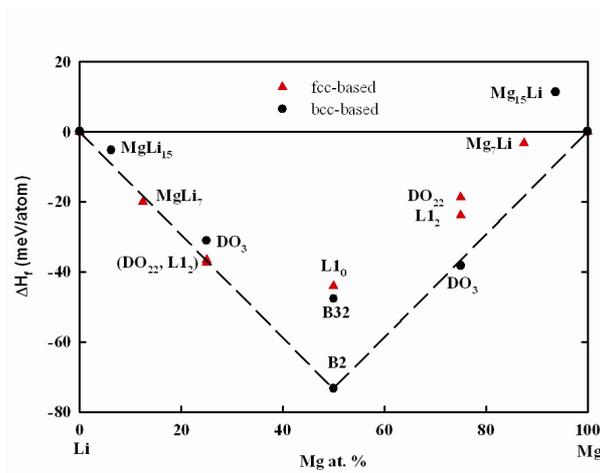

Fig. 1. Predicted heats of formation for Mg-Li alloys. The common-tangent construction for stability limits of the different phases is indicated by the dashed lines.
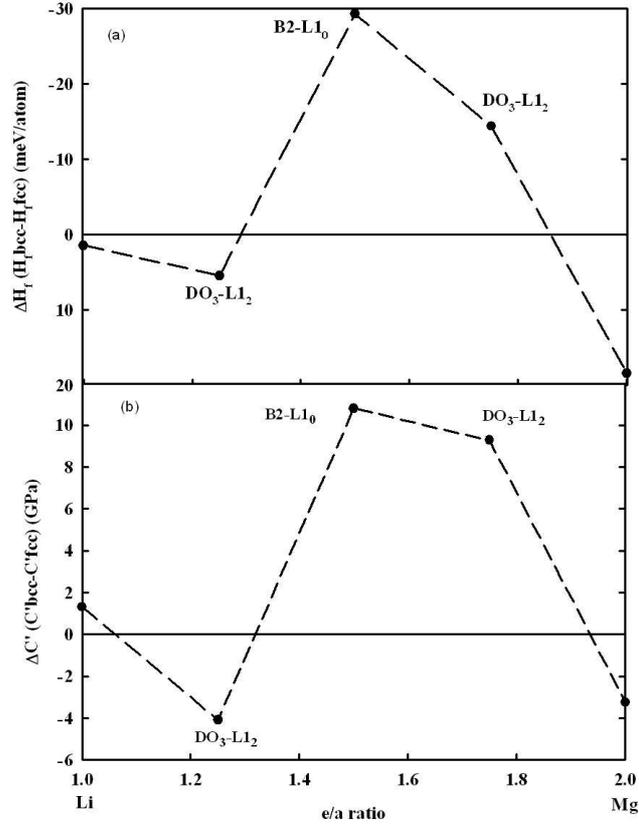
Fig. 2. (a) Structural formation energy differences, ΔH_f between corresponding bcc and fcc Mg-Li compounds, against the electron per atom ratio and (b) change in shear modulus between bcc and fcc superstructures. Note that the plot (a) has negative axis running vertically upwards to make comparison with (b) real.

3.2 Mechanical stability

The calculated elastic constants for the cubic Mg-Li alloys are listed in Table 1. The elastic constants of the fcc Mg lattice are in good agreement with the available theoretical results [22] while the bcc phase is found to be mechanically unstable, since the tetragonal shear modulus C' is negative. Our results for pure Li in both fcc and bcc lattices show mechanical stability with the elastic constants being in good agreement with both

11

experimental [23,24] and previous theoretical [25] results, except for the case of C_{11} and C_{44} of the bcc lattice which are overestimated. The elastic constants in Ref. 40 are derived from calculated phonon dispersions. Our predicted elasitic constants were calculated at equilibrium lattice constants rather than the experimental values, hence led to slight difference from experimentally determined elasticity. This may be ascribed to the elastic constants being sensitive to the lattice constant of the crystal [41].

Other elastic moduli such as shear modulus (G), Young's modulus (E), and B/G ratio of Mg-Li alloys are also listed in Table 1. Most of the elastic constants of Mg-Li structures listed in satisfy the mechanical stability criteria of cubic systems as outlined elsewhere [15,25,42] as follows:

$$C_{44} > 0, \ C_{11} > \left| C_{12} \right| \quad \text{and} \quad C_{11} + 2C_{12} > 0$$

except for Mg bcc, Mg_7Li, Mg_3Li (L1$_2$) and $MgLi_7$ structures which are mechanically unstable. These elastic stability conditions also lead to a restriction on the magnitude of B. Since B is a weighed average of C_{11} and C_{12} and stability requires that C_{12} be smaller than C_{11}, we are then left with the result that B is required to be intermediate in value between C_{11} and C_{12}: $C_{12} < B < C_{11}$.

There is a good agreement between the bulk moduli obtained from elastic constants as well as from equation of states with available experimental [26] and other previous theoretical results [9,18]. With increasing Li concentration, the bulk modulus decreased monotonically. Pugh proposed the B/G ratio to predict the ductility (> 1.75) or brittleness (< 1.75) [27]. For cubic Mg-Li alloys in Table 1, the B/G increases from very brittle (≤ 50 at.% Li) to ductile (> 50 at.% Li) with increasing Li composition. The bcc phases has maximum ductility at 75 at.% Li, while the same is achieved at 87.5 at.% Li for fcc Mg-

Li structures although accompanied by mechanically instability. The negative values of *B/G* also reflect instability of the corresponding compounds. As expected from thermodynamics, it is evident from Table 1 that the fcc phases at low Li content (< 50at.%) are mechanically unstable. It is also interesting to note that the bcc $Mg_{15}Li$ and DO_3 (Mg_3Li) structures are the only mechanically stable phases ($C_{11} > C_{12}$) in this Mg-rich region, although their *B/G* values is lower than 1.75, indicating brittleness, and hence have the highest Young's modulus *E*. This stability is in agreement with experiment, that in this composition range the bcc phase is mechanically stable, and coexist with the hcp phase [2,21]. However, in agreement with predictions by Counts et al [9], our results reveal brittleness between 25 and 50 at.% Li. Furthermore, at 50:50 composition we predict B2 to be the most stable phase compared to B32 but we note the opposite with regard to ductility, where B2 is brittle. The superiority of B32 in ductility is in agreement with results obtained in Ref. 9. At $MgLi_3$ composition, our elasticity results suggest the fcc phase to be the most mechanically stable than bcc, in agreement with Hafner's work [21] and experiment at low temperature, although bcc is still the most ductile than any other composition, in agreement with recent reports [9].

Besides *B/G*, it was recently found that the *C'* is also very significant on the mechanical properties of materials [43]. The mechanical stability can be quantified by calculation of the tetragonal shear modulus, *C'*. The *C'* for the bcc and fcc ordered phases is also listed in Table 1 and shown as a function of composition in Figure 3. The ordered fcc phases are mechanically unstable at 50 at.% Mg and above (Mg-rich), while for concentrations less than 50 at% Mg, the ordered bcc structures are either unstable or metastable compared to fcc. The elastically unstable structures showed negative Young's modulus.

As observed in Li-rich compositions, the smaller C' the lower the Young's modulus. This elastic behaviour in crystals has been reported to yield better plasticity [43,44].

Table 1. Predicted elastic constants of Mg-Li alloys at equilibrium lattice parameters. The bulk moduli determined from elastic constants is compared with the ones calculated from equation of states. Asterisks denote the results generated from this work. For comparison, theoretical and experimental results are shown in parentheses, normal and square brackets, respectively.

Comp.	Phase	a_0 Å	C_{11} GPa	C_{12} GPa	C_{44} GPa	B GPa	C' GPa	G GPa	$B = V_0 \frac{d^2E}{dV^2}$ GPa	B/G	E GPa	A
Mg	fcc*	4.530	42.8	31.0	23.1	34.9	5.9	13.4	34.1	2.60	35.7	1.8
	fcc	4.520[22]	46.0	27.4	30.0	33.6	9.3					
		4.516[37]										
	bcc*	3.585	25.6	39.4	36.0	34.8	-6.9	-5.4	37.6	-6.44	-1.7	4.3
		3.571[37]										
Mg$_{15}$Li	bcc*	3.568	55.8	24.7	50.9	35.1	15.5	31.7	32.9	1.11	73.1	1.7
Mg$_7$Li	fcc*	4.495	22.2	29.5	24.2	27.0	-3.6	0.6	34.0	45.00	1.8	3.5
Mg$_3$Li	L1$_2$*	4.458	25.8	29.9	24.5	28.5	-2.1	-2.9	27.2	-9.83	-9.0	3.1
									(29.4)[18]			
35%Li	DO$_3$*	3.512	40.0	25.6	41.0	30.4	7.2	20.9	32.8	1.45	51.0	2.7
	bcc[38]		35.1	24.4	26.4	28.0			(30.5)[18]			
									25.0			
MgLi	B2*	3.420	37.5	19.7	25.9	25.6	8.9	16.9	22.1	1.51	41.6	1.9
		3.458[36]							(20.2)[18]			
Exp[29]									27.5[36]			
	55%		32.2	19.8	26.6	23.9		-				
	45%		28.5	20.5	19.4	23.2		-				

14

	B32*	3.474	31.0	24.6	28.6	26.7	3.2	12.6	25.2	2.12	32.7	2.5
	L1$_0$*	4.820	25.4	29.2	24.8	22.3	-1.9	15.0	25.2	1.49	36.7	39.7
		c/a=0.72	C$_{33}$=15.3	C$_{13}$=19.1	C$_{66}$=27.0				(24.2)[18]			-14.2
MgLi$_3$	L1$_2$*	4.309	25.8	15.9	18.7	19.2	4.9	11.0	19.1	1.74	27.7	2.1
									(18.8)[18]			
	DO$_3$*	3.423	19.4	17.8	15.4	18.3	0.8	5.7	18.0	3.21	15.5	2.5
75%Li	bcc[38]		15.7	15.0	13.6	15.2			(18.8)[18]			
									15.0			
MgLi$_7$	fcc*	4.305	15.8	16.9	11.7	16.6	-0.6	2.7	16.4	6.15	8.2	2.5
MgLi$_{15}$	bcc*	3.421	18.2	13.2	11.5	14.9	2.5	6.3	23.1	2.36	16.5	2.0
Li	fcc*	4.307	17.5	11.4	9.3	13.4	3.0	6.0	13.9	2.23	15.7	1.7
Cal	fcc	4.321[37]	19.8[40]	13.6	10.9	15.7	-				14.0	2.7
	bcc*	3.424	19.6	10.9	16.1	13.8	4.4	9.6	12.0	1.44	23.4	2.2
Cal	bcc	3.442[37]	17.7[39]	13.4	10.0	14.8	2.0	-	15.2			
Cal	bcc		16.8[40]	13.0	11.0	14.3						
Exp.[24]	bcc[24]	3.491	14.8	12.5	10.8	13.3		-				

The corresponding structural shear modulus C' differences, $\Delta C'$, between bcc and fcc ordered Mg-Li compounds, against the electron per atom ratio ranging from 1 (Li) to 2 (Mg), relative to hcp Mg and Li lattices, are plotted in Fig. 2(b). We find an interesting correlation between these quantities, that, in the region where bcc is very stable compared to fcc, the shear modulus is positive for bcc but negative for fcc (i.e. the fcc lattice is mechanically unstable) and vice versa. A similar behaviour had been pointed out earlier for Ni-Cr disordered bcc and fcc phases by Craievich et al [30] and for B2 and L1$_0$ TiAl by Sob et al [31]. This reflects the underlying change in hcp to fcc to bcc to hcp structural

stability as the electron per atom ratio changes from 1 (Li) to 2 (Mg). In terms of the predicted phase stability trend, a common behaviour is found between the change in tetragonal shear modulus ($\Delta C'$) and formation energy differences of corresponding bcc and fcc ordered compounds relative to hcp Mg and Li lattices, which seems to correlate the two structural properties. However, since in the low concentration limit as well as for higher temperatures the effect of the chemical disorder on the elastic properties of Mg-Li alloys could be significant, some more work concerning the random fcc and bcc phases would require attention.

Another crucial elastic moduli considered to have a significant implication in engineering science is the elastic anisotropy of crystals, since it is reported to be highly correlated with the possibility to induce micro-cracks in the material [45]. For a completely isotropic material $A = 1$, while values smaller or greater than unity measure the degree of elastic anisotropy. As observed in Table 1, cubic Mg-Li alloys are generally anisotropic.
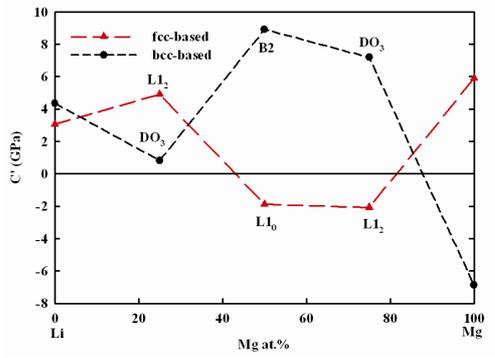

FIG. 3. Calculated Mg-Li elastic constants (tetragonal shear modulus) $C'=(C_{11}-C_{12})/2$ as a function of composition for ordered bcc and fcc phases.

3. 3 Electronic structure

The relation between structural stability and the behaviour of the electronic density of states (DOS) in the vicinity of the Fermi energy can be formalized by a Jones-type analysis [32]. Using a rigid-band model, the theory shows how structure in the density of states translates into an energy difference for competing phases as a function of the electron count. Within the rigid-band approximation we assume that the bands of hcp, fcc, and bcc lithium remain unchanged (or rigid) on alloying. A Jones-type analysis then states that the structural energy difference between any two lattices at the same atomic volume is given by

$$\Delta U = \Delta U_{band} = \Delta \left[\int^{E_F} E n(E) dE \right] \tag{2}$$

where $n(E)$ is the electronic density of state (DOS) per atom and E_F is the Fermi energy. The difference in the band energy ΔU_{band}, is calculated under the constraint that the potential within the Wigner-Seitz (WS) spheres remain unchanged on going from one structure-type to another. The band energy difference equation allows us to perform a Jones-type analysis that links the relative stability of the two structures to the relative behaviour of the corresponding DOS. This link results from the relationship between the Fermi energy, E_F, and the number of valence electrons, N, according to

$$N = \int^{E_F} n(E) dE \tag{3}$$

In order to understand the behaviour of the band energy difference, ΔU_{band}, we exploit the

following expressi

respect to the electr

$$\frac{d}{dN}(\Delta U_{band}) = \Delta\left[\frac{d}{d}\right.$$

$$\frac{d^2}{dN^2}(\Delta U_{band}) = \Delta\left[\right.$$

a maximum aroun

where the fcc DOS

lowest, whereas the

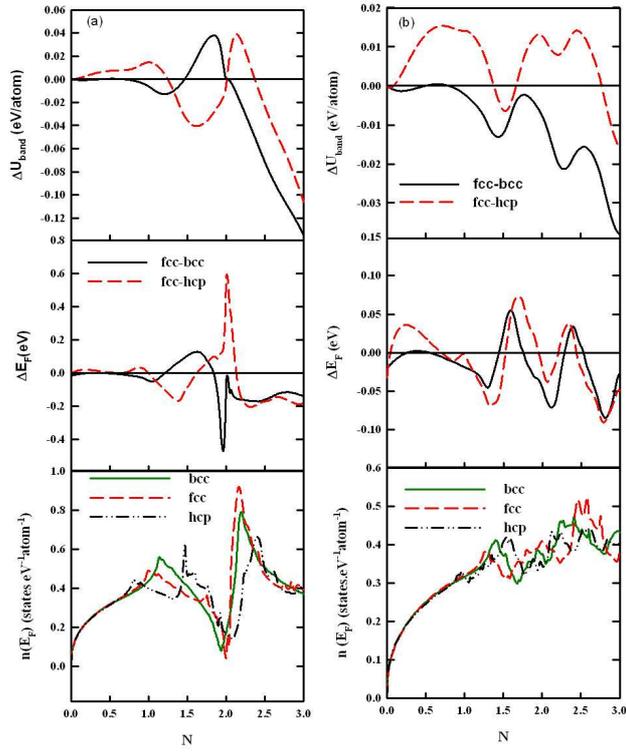lowest. The hcp st

is lowest. We see t

trend from (Li) hcp

Fig. 4. Analysis of fcc, bcc, and hcp relative structural stabilities within the rigid-band approximation for Mg-Li alloys. The difference in band energy ΔU_{band} with respect to elemental (a) Li and (b) Mg rigid bands, Fermi energies ΔE_F, and the density of states at the Fermi level E_F for bcc, fcc, and hcp lattices, are plotted as a function of band filling, N.

4. Conclusions

Using *ab initio* technique, the phase stability of cubic Mg-Li alloys has been predicted from heats of formation and elasticity, both complementing each other. The observed stability trend (Li) hcp → fcc → bcc → hcp (Mg) has also been confirmed by the Jones-type analysis based density of states due to electron band filling. On the basis of established phase stability, the existence of cubic Mg-Li alloys in chosen compositions is validated. In terms of the predicted phase stability trend, a common behaviour is found between the change in tetragonal shear modulus ($\Delta C'$) and formation energy differences of corresponding bcc and fcc ordered compounds relative to hcp Mg and Li lattices, which seems to correlate the two structural properties. The ductility of cubic phases improves with increasing Li concentration, although at the expense of monotonically decreasing bulk modulus. Furthermore, increasing Li content results in smaller C' and thus lower Young's modulus, meanwhile yielding better plasticity.

Acknowledgements

References

[1] E.F. Emiley, in "Principles of Mg technology" (Pergamon Press, Oxford, 1966).

[2] T.B. Massalski (Ed.), Binary Alloy Phase Diagrams, ASM International, Metals Park (OH), 1992.

[3] S. Curtarolo, A.N. Kolmogorov, and F.H. Cocks, CALPHAD **29** (2005) 155.

[4] T. Uesugi and K. Higashi, Mater. Sci. Forum **488-489** (2005) 131.

[5] F. Ducastelle, "*Order and Phase Stability in Alloys*", Cohesion and Structure series, Vol. **3**, ed. By F.R. de Boer and D.G. Pettifor (North-Holland, Amsterdam, 1991).

[6] P.E.A. Turchi, "*Electronic Theories of Alloy Stability*", in Intermetallic Compounds: Principles and Practice, Vol. **1**, Chap. 2, ed. By J.H. Westbrook and R.L. Fleischer (John Wiley & Sons, Ltd., New York, 1995).

[7] T. Uesugi, M. Kohyama, M. Kohzu and K. Higashi, Mater. Sci. Forum, **350-351** (2000) 49.

[8] T. Uesugi, M. Kohyama, M. Kohzu and K. Higashi, Mater. Trans., **42** (2001) 1167.

[9] W.A. Counts, M. Friák, D. Raabe and J. Neugebauer, Acta Mater., **57** (2009) 69.

[10] V. Milman, B. Winkler, J.A. White, C.J. Pickard, M.C. Payne, E.V. Akhmatskaya and R.H. Nobes, Int. J. Quantum Chem. **77** (2000) 895.

[11] P. Hohenberg and W. Kohn, Phys. Rev. **136**, **B** 864 (1964), W. Kohn and L.J. Sham, Phys. Rev. **140** (1965) **A** 1133.

[12] J.P. Perdew and Y. Wang, Phys. Rev. **B 45** (1992) 13244.

[13] J.P. Perdew, K. Burke and M. Krnzerhof, Phys. Rev. Lett. **77** (1996) 3865.

[14] D. Vanderbilt, Phys. Rev. **B 41** (1990) 7892.

[15] M.J. Phasha, MSc thesis submitted to the School of Physical and Mineral Sciences, University of Limpopo (formerly "of the North") in 2005.

[16] H.J. Monkhorst and J.D. Pack, Phys. Rev. **B 13** (1976) 5188.

[17] M.D. Segall, P.L.D. Lindan, M.J. Probert, C.J. Pickard, P.J. Hasnip, S.J. Clark and M.C. Payne, J. Phys. Cond. Matt. **14** (2002) 2717.

[18] H.L. Skriver, Materials Science Databases, CAMP, DTU, http://databases.fysik.dtu.dk/.

[19] D.W. Levinson, Acta Met., **3**(1955) 294.

[20] F.H. Herbstein and B.L. Averbach, Acta Met., **4** (1956) 407.

[21] J. Hafner, J. Phys. **F 6** (1976) 1243.

[22] A. Zhu, B.M. Gable, G.T. Shiflet and E.A. Starke Jr., Acta Mater. **52** (2004) 3671.

[23] R. A. Felice, J. Trivisonno, D. E. Schuele, Phys. Rev. **B 16** (1977) 5173.

[24] G. Simmons and H. Wang, Single Crystal Elastic Constants and Calculated Aggregate Properties: A handbook, 2nd ed. (MIT Press, Cambridge, Massachusetts, 1971).

[25] M.J. Mehl, B.M. Klein, and D.A. Papaconstantopoulos, Intermetallic Compounds: Vol. 1, Principles. Edited by J.H. Westbrook and R.L. Fleischer, 1994, John Wiley & Sons Ltd.

[26] R.W. Lynch and L.R. Edwards, J. Appl. Phys., **41** (1970) 5135.

[27] S.F. Pugh, Philos. Mag. **45** (1954) 823.

[28] R. Hill, The elastic behaviour of a crystalline aggregate. Proc. Phys. Soc**. A 65** (1952) 349.

[29] V.P. Mashkovetz and L.V. Puchkov, Zh. Prikl. Chem., (1965) 1875.

[30] P.J. Craievich and J.M. Sanchez, Comp. Mat. Sci. **8** (1997) 92.

[31] M. Sob, L.G. Wang and V. Vitek, Comp. Mat. Sci. **8** (1997) 100.

[32] H. Jones, Proc. Phys. Soc. A, **49** (1937) 250.

[33] O.K. Andersen, Phys. Rev. **B 12** (1975) 3060.

[34] O.K. Andersen, O. Jepsen and M. Sob, Electron Band Structure and its Applications, edited by M. Yossouff, Springer-Verlag, Berlin, 1987.

[35] H.L. Skriver, The LMTO method (Springer-Verlag, Berlin, 1984).

[36] B.R. Sahu, Mater. Sci. Eng. **B49** (1997) 74.

[37] Y.Wang, S. Curtarolo, C. Jiang, R. Arroyave, T. Wang, G. Ceder, L.-Q. Chen and Z.-K. Liu, Calphad-Computer Coupling of Phase Diagrams and Thermochemistry **28** (2004) 79.

[38] P. Beauchamp, R. Taylor and V. Vitek, J. Phys. F. Metal Phys. **5** (1975) 2017.

[39] A. Razaque, AK.M.A. Islam, F.N. Islam and M.N. Islam, Solid State Commun. **131** (2004) 671.

[40] R. Taylor and A.H. MacDonald, J. Phys. F: Metal Phys. **10** (1980) L181.

[41] Y. Sun and E. Kaxiras, Phil. Mag. **A 75** (1997) 1117.

[42] J.F. Nye, Physical Properties of Crystals, Oxford University Press, Oxford, 1985.

[43] Q.M. Hu and R. Yang, Curr. Opin. Solid St. Mater. Sci. **10** (2006) 19.

[44] B.Y. Tang, W.Y. Yu, X.Q. Zeng, W.J. Ding and M.F. Gray, Mater. Sci. Eng. **A 489** (2008) 444.

[45] S. Goumri-Said and M.B. Kanoun, Comput. Mater. Sci. **43** (2007) 243.